Computer simulations of auxetic foams in two dimensions

2013 Smart Mater. Struct. 22 084009

(http://iopscience.iop.org/0964-1726/22/8/084009)

IOP Publishing Smart Materials and Structures
Smart Mater. Struct. **22** (2013) 084009 (11pp) doi:10.1088/0964-1726/22/8/084009

Computer simulations of auxetic foams in two dimensions

A A Pozniak[1], J Smardzewski[2] and K W Wojciechowski[3]

[1] Department of Technical Physics, Poznań University of Technology, Nieszawska 13A, 60-965 Poznań, Poland
[2] Department of Furniture Design, Faculty of Wood Technology, Poznań University of Life Sciences, Wojska Polskiego 38/42, 60-627 Poznań, Poland
[3] Institute of Molecular Physics, Polish Academy of Sciences, M. Smoluchowskiego 17, 60-179 Poznań, Poland

E-mail: kww@ifmpan.poznan.pl

Received 24 May 2013, in final form 11 June 2013
Published 22 July 2013
Online at stacks.iop.org/SMS/22/084009

Abstract
Two simple models of two-dimensional auxetic (i.e. negative Poisson's ratio) foams are studied by computer simulations. In the first one, further referred to as a Y-model, the ribs forming the cells of the foam are connected at points corresponding to sites of a disordered honeycomb lattice. In the second one, coined a Δ-model, the connections of the ribs are not point-like but spatial. For simplicity, they are represented by triangles centered at the honeycomb lattice points. Three kinds of joints are considered for each model, soft, normal and hard, respectively corresponding to materials with Young's modulus ten times smaller than, equal to and ten times larger than that of the ribs. The initial lattices are uniformly compressed, which decreases their linear dimensions by about 15%. The resulting structures are then used as reference structures with no internal stress. The Poisson's ratios of these reference structures are determined by stretching them, in either the x or the y direction. The results obtained for finite meshes and finite samples are extrapolated to infinitely fine mesh and to the thermodynamic limit, respectively. The extrapolations indicate that meshes with as few as 13 nodes across a rib and samples as small as containing 16×16 cells approximate the Poisson's ratios of systems of infinite size and infinite mesh resolution within the statistical accuracy of the experiments, i.e. a few per cent. The simulations show that by applying harder joints one can reach lower Poisson's ratios, i.e. foams with more auxetic properties. It also follows from the simulations performed that the Δ-model gives lower Poisson's ratios than the Y-model. Finally, the simulations using fine meshes for the samples are compared with the ones in which the ribs are approximated by Timoshenko beams. Taking into account simplifications in the latter model, the agreement is surprisingly good.

(Some figures may appear in colour only in the online journal)

1. Introduction

Typical foams are low density, cellular materials revealing interesting and useful properties, and, thus, finding a vast number of applications [1]. Foams can be made of various materials. The most common are polymer and metallic ones; however, foams made of glass and ceramics are also known [1].

The structures of foams are usually highly disordered. For this reason, approaches based on simple, periodic structures are unrealistic and clearly insufficient for precise description of such complex systems. Computer simulations constitute a tool which allows for effective, quantitative investigations of various complex systems. Moreover, computer experiments can be carried out without material specimens and laboratory equipment. In consequence, numerical approaches can overcome many limits typical for experimental approaches,

thus allowing easy introduction of numerous modifications, e.g. structural and topological changes or varying material properties. The analysis process itself may be precisely tuned by manipulating boundary conditions, load rate, etc. Obviously, the power of computer simulations is not unlimited and various problems remain big challenges. For instance, the finite element method (FEM), which has become a mature and easily available method, is still not suited for modeling extremely large deformations and contact handling [2].

A field of increasing interest, in both technology and science, is the compressive behavior of foams. During compression, foams undergo certain transformations, depending on the level of compressive strain. Foam structures can behave differently for uniaxial, biaxial or three-axial compressions. There exist theoretical models describing the behavior of struts (open-cell) and sheets (closed-cell) [1]. The compressive behavior has been a subject of intensive investigation by both experimental [3–6] and numerical [2, 7–10] methods. Analytical considerations for compression of three-dimensional foam were presented in the work by Zhu *et al* [11, 12]. In their more recent work [13, 14] the FEM approach was applied. The compressive response of open-cell foams was also discussed by Gong and co-workers [15, 16]. Roberts and Garboczi have studied the compression of closed-cell [17] and open-cell models [18]. An interesting approach exploiting variants of the material point method was presented by Brydon *et al* [2, 19]. Micro-tomographic imaging of an open-cell foam analysis is given in the paper by Elliot *et al* [20]. Recent studies of the compressive behavior of foams have been conducted by McDonald *et al* [5], where precise spatial x-ray imaging was presented. In a following paper [9] these authors presented numerical simulations based on the model obtained from three-dimensional x-ray imaging.

It has been shown by Lakes [21] and later by Grima [22] that a conventional polymeric foam first subjected to a compression procedure and then unstressed and stabilized by a proper thermal [21] or chemical [22] treatment converts into a material of unconventional (*negative*) Poisson's ratio. (The Poisson's ratio is the negative ratio of the relative change of transverse dimension of a longitudinally stretched or compressed body to a relative change of its longitudinal dimension [23]. For anisotropic bodies the Poisson's ratio can depend on both the longitudinal and transverse directions.) Models and materials with such an unusual property, coined *auxetics* by Evans [24] have been studied by many researchers [10, 25–60]. The main reason for the rapidly growing interest in these systems is their various counterintuitive properties [61, 62] which offer a broad range of possible applications, including those typical for smart materials [63–68].

Following Lakes [21], the origin of the negative Poisson's ratio phenomenon is generally attributed to the structure conversion during compression. More discussion on this subject can be found in papers by Lakes, Grima, Scarpa, Smith, and others [69–77]. The present work concerns the two-dimensional (2D) version of this subject.

Although the three-dimensional (3D) topology is richer than the 2D one, 2D systems can be used as a good starting point for the investigation of properties of foams. This is so because 2D structures can be simulated with less computational power, i.e. computer memory and CPU time, and the obtained results are easier to analyze because of the possibility of visual inspection of the structures obtained and their defects. Analysis of the processes of forming common foams suggests that the simplest model of 2D foam would be a honeycomb structure based on a hexagonal lattice. Two-dimensional honeycombs explicitly reveal the close connection between the microstructure and the mechanical properties [1]. In particular, auxetic honeycombs present the link between the structure and the (negative) sign of the Poisson's ratio. The mechanical behavior of negative Poisson's ratio (NPR) honeycombs was presented in work by Scarpa *et al* [78] and Gaspar *et al* [79]. In the recent work by Elipe and Lantada [80] a variety of auxetic honeycombs are presented.

Despite the fact that auxetic materials have been known for more than two decades, there still remain many important questions to answer. One of the challenges is to establish precisely the role of various mechanisms leading to auxetic behavior of converted foams. Another one is a search for mechanisms leading to extremely negative values of the Poisson's ratio. These issues are not only important from the scientific point of view but are also crucial for the technology. These are complex problems as the specimen can undergo various modifications, material and structural. Quantitative studies of properly selected models can help to solve these problems.

This paper is focused on the conversion of common foam structures into auxetic structures. Two models are considered, which have their origin in two facts known in the literature. (1) The first fact is that the Poisson's ratio must be equal to -1 (which is its minimum value in unconstrained, stable, isotropic materials of dimensionality two and higher) if the angles between foam *nodes* (i.e. the places where the *ribs* forming the structure are joined with each other) are fixed [32, 54]. This model is further referred to as the perfectly *rigid joints model*. (2) The second fact is the possibility of obtaining the same, minimum value of the Poisson's ratio in a model with nodes that are not point-like but circular and can rotate, as proposed by Lakes [31]. The latter *rotating node model* (which can be seen as a particular case of an earlier, rigorously solved model [28] of negative Poisson's coefficient) has been studied by many researchers [38, 81–83]. The models considered in this paper incorporate both the mechanism of joints of variable rigidity and rotating nodes of variable rigidity and size. The aim of this preliminary study is to compare the two mechanisms when neither the joints are rigid nor the nodes are circular.

The paper is organized as follows. In section 2, the two models of 2D isotropic foam studied in this work are presented. The numerical procedure for solving the models is sketched in section 3 where also the choice of the optimal parameters (size, disorder, mesh) of the model and the solving procedure are discussed. In section 4, the obtained numerical results are described and interpreted. Finally, in section 5, outcomes are summarized and conclusions are drawn.

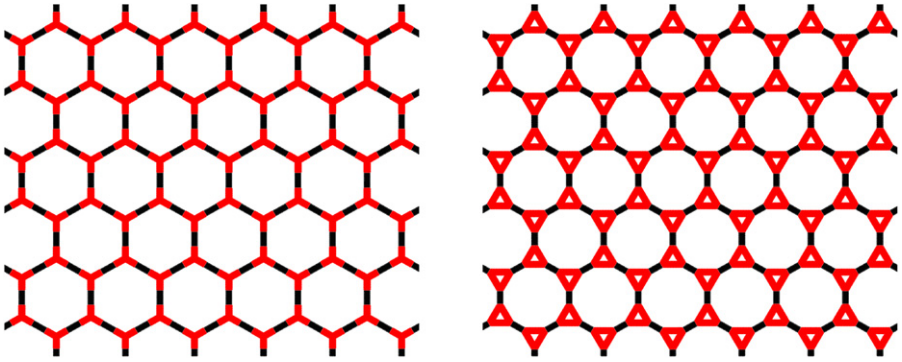

Figure 1. (a) Honeycomb (Y-model) and (b) kagomé-like (Δ-model) periodic structures.

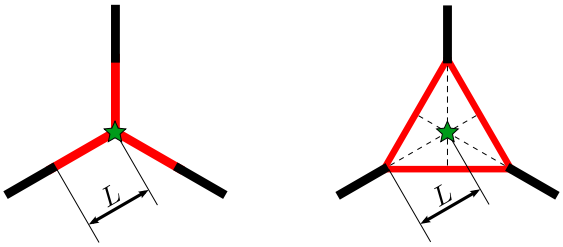

Figure 2. Two types of joints, called Y-joints and Δ-joints, used, respectively, in the Y-model (left) and the Δ-model (right). The parameter L characterizes the size of the weakened or reinforced region and determines the size of the (Y and Δ) joints (marked in red in the on-line version). The stars (green in the on-line version) represent s-nodes. By definition, the dashed lines, being extensions of the ribs in the Δ-joints (right), always cross each other in s-nodes of the Δ-structure.

2. The models

In figure 1(a) a 6 × 6 sample of a perfect honeycomb structure is shown. The nodes of this structure (*s-nodes*) are the places in which the lattice sides (further referred to as *ribs*) are connected with other ribs. In figure 1(b) a kagomé-like structure is shown, which is obtained from the honeycomb one by replacing the Y-like joints by the Δ-like joints presented in figure 2. In the latter case the s-nodes will be identified with the 'centers' of the triangles in which the extensions of the ribs cross each other.

Both of the periodic structures shown in figure 1 are clearly isotropic as they show six-fold symmetry axes perpendicular to the plane [23]. At first sight it might seem that to obtain isotropic auxetic foams one could apply to the structures shown in figure 1 the numerical procedure corresponding to those exploited either by Lakes [21] or by Grima [22], i.e. uniform compression and then relaxation. However, such an approach is improper for the reasons pointed out below.

(1) The first reason is that during uniform biaxial compression of honeycomb or kagomé-like structures, they buckle in the modes presented in figure 3. In fact, some minimal disorder ($f = 0.001$, for the definition of f see the text below) was introduced to the periodic structures shown in figure 1, to eliminate their translational degeneracy. (A comprehensive study of buckling modes in honeycombs under various circumstances may be found in [84].) The unwanted feature of the obtained structures is their *anisotropy*, which is easy to notice by visual inspection. The anisotropy can be confirmed by quantitative analysis of deformations caused by uniaxial stress applied in the x and y directions.

(2) The second reason is that the structures shown in figure 1 are *too small* to sample the properties of homogeneous foam properly. This will be clearly seen from discussion of the results presented in section 3.

(3) The third reason is that *boundary conditions* are not specified.

Thus, it is necessary to introduce certain modifications of the initial structure to fulfil the isotropy and homogeneity of an auxetic foam. A simple way to reach isotropy *after* compression is by introducing *disorder* to the initial structure. This can be done in various ways. In this work uniform structural disorder was obtained by moving each s-node (see figure 2) randomly within a circle centered at a perfect-lattice position of the site. The circle radius defines the maximum amplitude of s-node movements. Obviously, when the amplitudes of the movements are not too large (i.e. the neighboring circles do not overlap), the topology of the initial lattice remains unchanged, i.e. each vertex has the same neighbors as in the case of perfectly ordered structure. Assuming that the initial distance between s-nodes is D, a random number generator was used to move the s-nodes within a circle of radius equal to $f \cdot D$, where $f \in \langle 0, 0.5)$. This value range prevents the system from topology changes.

Remark. The distances between neighboring s-nodes after their movements are further denoted by d. Obviously, in the disordered structure, d depends on the numbers of neighboring nodes, e.g. i and j, and one might prefer to denote the distances by d_{ij}. In this paper, however, these lower indices are avoided, to shorten the notation.

The lengths of joints in the disordered lattice are defined by the condition $l/d = L/D$. In this paper only the case with

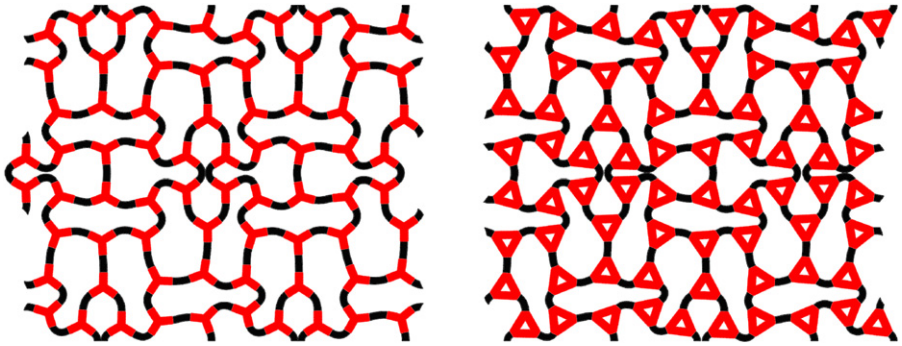

(a) (b)

Figure 3. The structures shown in figure 1 uniformly compressed by 20% of their linear dimensions: (a) Y-model, (b) Δ-model.

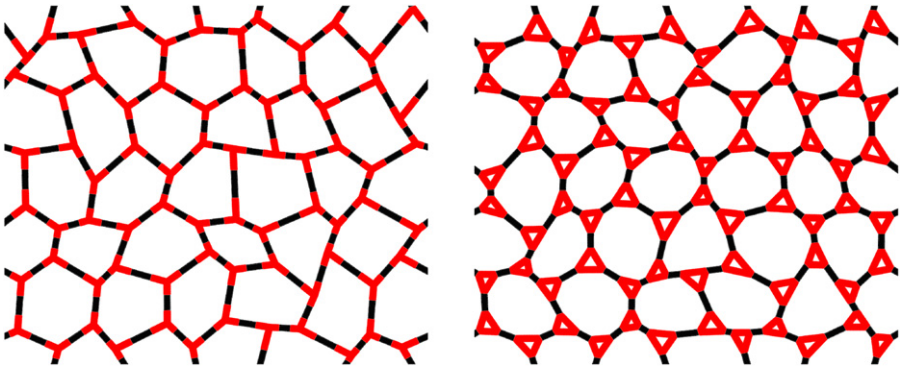

(a) (b)

Figure 4. 6×6 samples of structures with disorder parameter $f = 0.45$: (a) Y-model, (b) Δ-model.

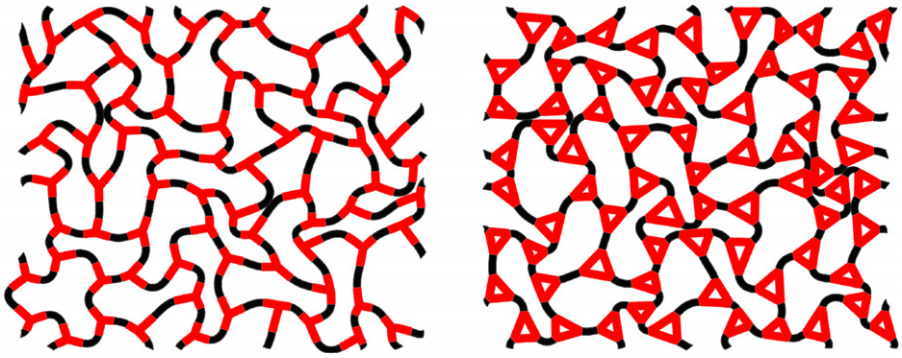

(a) (b)

Figure 5. The structures shown in figure 4 uniformly compressed by 20% of their linear dimensions: (a) Y-model, (b) Δ-model.

$L/D = 0.3$ is considered. It should be added that the thickness of all the ribs is equal to $0.15D$. To avoid the case when $l = 0$, it is convenient to slightly reduce the maximum value of f. Figure 4 presents the case of a disorder parameter $f = 0.45$ being introduced to the structures shown in figure 1. This is the largest disorder parameter used in this work and in figure 5 corresponding compressed structures are shown.

Remark. Taking into account the definition of the s-nodes, see figure 2, the way in which disorder is introduced to the kagomé-like lattice is the same as in the case of the honeycomb lattice.

The disorder introduced to the initial structures helps also in the homogeneity aspect. In figure 6 a structure of size 16×16 is presented. In general, as the disorder parameter increases, the sizes of the domains related to particular buckling modes are smaller. To obtain homogeneous (and isotropic) structures, the size of the model should be (much) larger then the correlation length (i.e. typical domain size). The presence of many randomly oriented domains leads to a homogeneous and isotropic structure. The size of the domains can be estimated by looking at the deformed structures, while a quantitative isotropy check can be made, e.g., by comparing

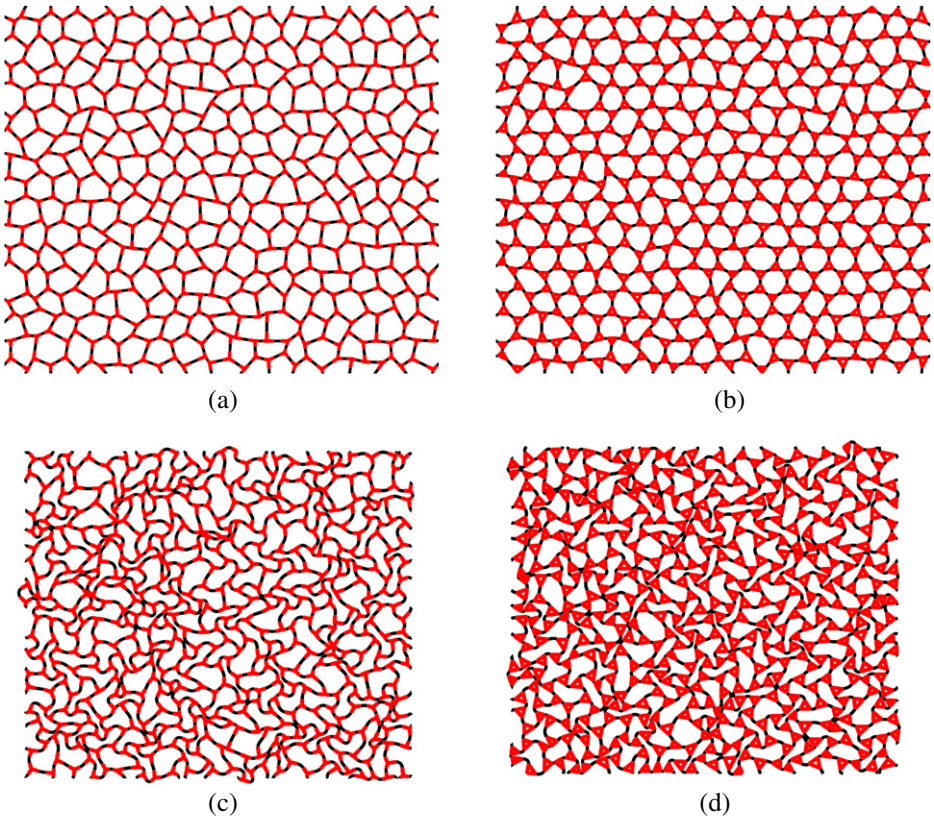

Figure 6. Disordered Y and Δ structures of size 16×16 in their ((a), (c)) initial and ((b), (d)) 20% compressed states. The parameter of disorder is $f = 0.45$.

the Poisson's ratios measured during stretching of the system along the x-axis and y-axis, respectively.

To study the effects of material modifications, the red parts (in the on-line version, see figures 1 and 4) of the joints are given one of three different values of Young's modulus, while the material properties of the black parts remain unchanged. The Young's modulus for the black elements of the structure is equal to 4.50 MPa, the Poisson's ratio reads 0.45, and the density equals 1200 kg m^{-3}. (These numbers correspond to flexible polyurethane [1].) The Young's modulus of the red parts takes values from the set $\{0.45,\ 4.50, 45.00\}$ MPa; these values are referred to as soft joints (SJs), normal joints (NJs), and hard joints (HJs), respectively. The motivation leading to hardening and increasing the area of joints is due to the fact [32, 54] that systems preferring conservation of angles between ribs at joints during deformation have, in general, lower Poisson's ratio.

It follows from the definition of the ordered structures and the way in which the disorder was introduced that the box of periodicity for the initial structures was a rectangle of bottom length $nD\sqrt{3}$ and height $3nD/2$, where n is the number of unit cells along the horizontal direction. During biaxial compression the box size was uniformly decreased, i.e. the box shape (the ratio of box sides) was kept fixed. The boundary conditions were similar to the standard periodic ones but slightly stronger. Selected nodes of the mesh (chosen as centers of the cuts of the ribs of the initial disordered structure by the initial box sides on the left and bottom sides of the rectangular periodic box) were subjected to the roller-type condition. The mesh nodes are further referred to as *m-nodes*. Thus, the extra restriction with respect to the standard periodic boundary conditions was that the selected m-nodes at the bottom side and left side were co-linear and always had the same (equal to zero) ordinates and abscissas, respectively. The corresponding m-nodes at the top and right were the periodic images of the selected bottom and left m-nodes, respectively. They were moving with very small speeds, to make the process quasi-static. During deformations, all the selected top m-nodes and right m-nodes had equal ordinates and abscissas, respectively.

Remark. It should be noticed that, in general, the existence of the additional constraint in the boundary conditions may be the source of residual stresses in the system. The influence of these residual stresses on the Poisson's ratio estimates, however, is expected to be small in the present simulations—not exceeding their statistical error. This is because the Poisson's ratio of the system in the thermodynamic limit should not depend on the boundary conditions applied and, as is shown in section 3, the models studied in this paper were large enough, in the sense of approximating the thermodynamic limit within the statistical error.

Stretching of the samples was carried out as follows. The system kept its periodicity while being stretched. The

abovementioned selected m-nodes at left and bottom were subjected to the roller-type condition. When stretching along the x axis, the selected m-nodes at the right boundary were moving slowly with the same (positive) horizontal component of velocity. The selected m-nodes at the top were moving in such a way as to keep equal ordinates and zero value of the vertical stress. When stretching along the y axis, the selected m-nodes at the top boundary were moving slowly with small speed and their vertical components of velocity were equal and positive. The selected m-nodes of the right-hand side of the box were moving in such a way as to have equal abscissas while keeping zero value of the horizontal stress.

3. The method of solution

The elastic problem considered is nonlinear. Despite the fact that the linear (Hookean) elastic material model is utilized, there are two aspects leading to strong nonlinearities, i.e. *large displacements* and *contacts* between ribs. Respecting these elements in the simulations is crucial in order to properly model the behavior of foam for severe compression levels. The authors are aware that applying the Hookean material is a serious simplification; however, it is precise enough for the initial studies of the structure's Poisson's ratio. Further, a nonlinear constitutive law would be a new source of system nonlinearity, which would certainly make the system harder to solve. The Green–Lagrange tensor [23] is considered in the analysis,

$$\epsilon_{ij} = \left(\frac{\partial u_{\mathrm{i}}}{\partial x_j} + \frac{\partial u_j}{\partial x_{\mathrm{i}}} + \frac{\partial u_k}{\partial x_{\mathrm{i}}} \frac{\partial u_k}{\partial x_j} \right),$$

where u_{i} stands for the displacement vector component and x_{i} denotes the initial coordinates.

Remark. The symbol ϵ above should not be confused with the ε denoting engineering strain in figures 9–11.

In order to perform the computations defined in the previous section, Abaqus (version 6.10) [85] was used as the general framework providing all of the required features, e.g. general automated contact within large displacements. A Python scripting interface was applied extensively for automation of simulations. A very useful, time-saving feature of Abaqus/STANDARD was its possibility to deal with the contact mechanics automatically, without the necessity to define master–slave surfaces manually.

Since strongly disordered systems were considered, the representative volume element (RVE) scheme was used. Additionally, the system was enriched with the boundary conditions defined in the previous section, which is non-standard procedure within the RVE treatment. The idea of the RVE-based computational scheme is to select a structure that is large enough to treat it as statistically homogeneous. A discussion concerning the RVE-based approach in bifurcating microstructures may be found in [86].

The simulations consisted of two steps. The first one was (i) *uniform biaxial compression* and stress removal to convert a common foam into a compressed (auxetic) one. The second one was (ii) *uniaxial stretching* of the compressed (but stress-free) structure, to obtain the Poisson's ratio of the modified structure. Simulation of both steps was performed using a dynamic procedure utilizing the quasi-static approach, in which the inertial terms are negligible. The solver used was an implicit dynamic solver, a part of the Abaqus/STANDARD program. It handles the general contact for plane stress elements. The results obtained with the quasi-static approach were compared to those obtained with a static algorithm, in which the time variable was eliminated, and excellent agreement was obtained. The quasi-static solver was used in most of the simulations as it was much more efficient and allowed higher levels of compression to be obtained.

Facing the choice of the particular method of solution, two approaches are generally possible. The first one is a faithful mapping of the material geometry onto the FEM geometry. Then each rib and each joint of the abstract honeycomb or kagomé-like graph (see figure 1 or 4) is given a real thickness and after meshing is represented by a set of plane stress elements (CPS3 in Abaqus terminology), see figure 7(a). (As mentioned before, the thickness of the ribs was chosen to be $0.15D$ for all structures in the simulations discussed in this work.) The second approach utilizes a Timoshenko beam formalism (B21 in Abaqus terminology). The geometry is represented by wire elements (one-dimensional) and the physical thickness is later assigned by the solver.

The geometry and the mesh for step (ii) were obtained directly from step (i) by using the function *orphan mesh* (Abaqus/CAE feature), which returns the deformed geometry. Applying the function *orphan mesh* one obtains a deformed mesh as well, which may be in extreme cases substantially distorted. In order to avoid these problems, fine meshes were introduced at the first (compressive) step. This approach was chosen as the time cost of re-meshing of each structure between consecutive steps was too high.

The advantages of using one-dimensional elements (based on the formalism of the Timoshenko beam) include faster model generation (merging geometry), lower computational costs (in terms of memory and CPU consumption) and, finally, much smaller size of output databases. A serious disadvantage is that the B21 model does not take into account new contacts appearing between the buckling ribs (they 'penetrate' mutually instead of 'touching'). However, as will be seen in section 4, for low and mild compression levels this model can be useful, at least for quick (by about two orders of magnitude faster for typical runs) and low memory (by about one order of magnitude smaller for typical runs) estimates of Poisson's ratios.

The Poisson's ratio was calculated mainly in a geometrical manner, i.e. the negative ratio of lateral to longitudinal strains was computed. For some structures elastic constants were also calculated, from which Poisson's ratio values were obtained. Comparison of both approaches showed excellent agreement.

Remark. All the results presented in this work concern the differential Poisson's ratio. This means that for each time t_n, the reference state is the previous one, at t_{n-1}.

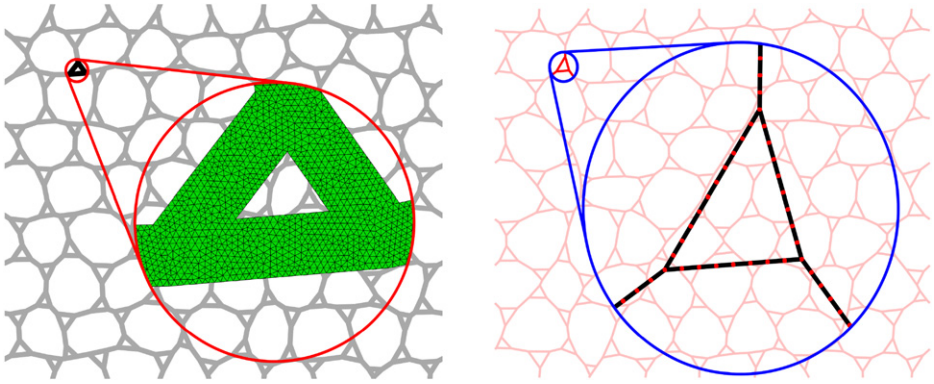

(a) (b)

Figure 7. Visualization of the difference between the same structure in two different versions: (a) the plane stress based and (b) the beam based approach. Although the elements in (b) are purely one-dimensional, the Abaqus solver assigns the desired finite width automatically. The red dots in (b) denote mesh nodes.

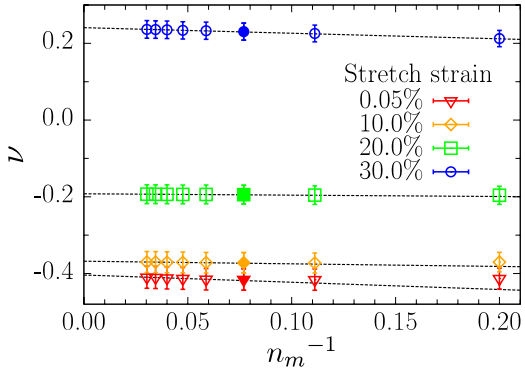

Figure 8. Convergence of the Poisson's ratio for a 4 × 4 NJ highly disordered ($f = 0.45$) system for various numbers of m-nodes across the rib. The values of the Poisson's ratio were averaged over the results taken from stretching along the x and y axes. The filled symbols represent the mesh density corresponding to $n_{\mathrm{m}} = 13$ points across the rib, used for further analysis.

Before starting simulations which produce results characterizing a macroscopic system (i.e. the thermodynamic limit of a microscopic sample) it is necessary to answer, at least, two questions. (1) How fine should the mesh be to guarantee proper results of the simulations? (2) How large should the studied samples be?

The first of the questions was answered by studying various meshes for disordered systems consisting of 4 × 4 unit cells. In figure 8 it can be seen that if there are $n_{\mathrm{m}} = 13$ m-nodes across a rib (the full symbols in figure 8 represent this number) then the difference between the obtained value of the Poisson's ratio and its value extrapolated to $n_{\mathrm{m}} \to \infty$ is less than 5%. Similar results were obtained for other systems.

To establish the proper size of the simulated samples one should take into account that, on one hand, they should be large enough to be homogeneous and isotropic and, on the other hand, small enough to allow for a sufficient number of runs. A larger number of runs results in more accurate averages and better estimates of their standard errors. The structures containing 8 × 8 unit cells, as the initial guess for the system size, appeared to be too small to be treated as statistically homogeneous and isotropic. Figure 9 shows the results for different $n \times n$ samples, where n varies from 12 to 24. The thick, black lines in each plot denote the result extrapolated to the thermodynamic limit. These were calculated by performing linear extrapolation with respect to $1/n$. It can be seen that the lines are within the error bars presented in the figures. The latter were calculated for the samples with $n = 16$, which turned out to be the optimal compromise between statistical accuracy and computational effort.

4. Results

In figure 10 the Poisson's ratio for foams simulated using the plane stress elements scheme is presented. All the structures are auxetic. Each compressed and relaxed structure was stretched twice, first along the x axis and secondly along the y axis. In the legend these situations are denoted as XX and YY respectively (a single Y might be confused with the Y symbol standing for the joint type). It can be seen that at large stretches (of amplitude exceeding half of the linear compression amplitude applied to transform a common foam into an auxetic one) the Poisson's ratios corresponding to stretching in the y-direction are higher than those corresponding to stretching in the x direction. As this result is qualitatively similar to the results obtained for structures with very small disorder ($f = 0.001$), one can interpret it as an indication of a 'residual' anisotropy caused by the lack of topological disorder. As the differences in the Poisson's ratios computed for stretching the samples in the x and y directions are not large, it is meaningful to approximate the Poisson's ratios of isotropic structures by their mean values. This approach was applied to the data presented in figure 11.

It can be also seen in figure 10 that harder joints lead to lower effective Poisson's ratios. Such a behavior

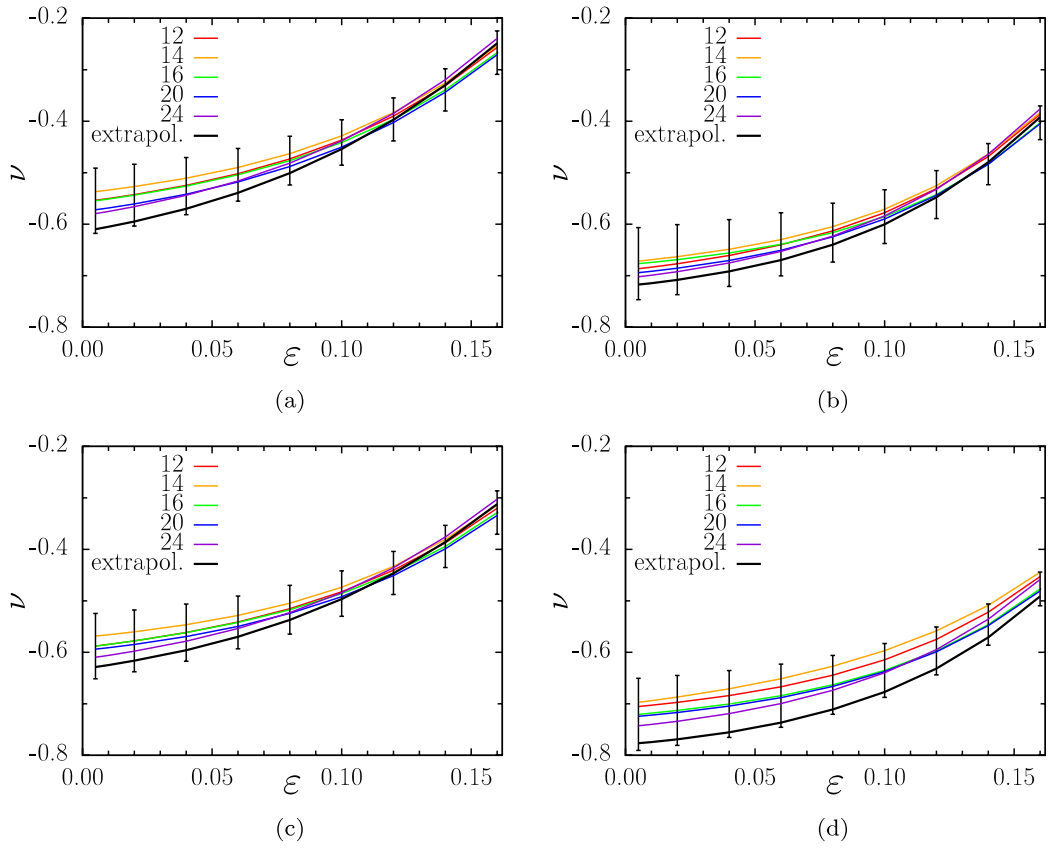

Figure 9. Convergence tests. The black line represents, at each strain, linear extrapolation of the average Poisson's ratio at a given inverse size to zero inverse size, taking $1/n$ as an argument when fitting. The statistical errors, shown for some strains for $n = 16$, indicate that for these strains the thermodynamic limit is, within the experimental error, equal to a few per cent. The numbers of structure cells and mesh elements for the structures numbered by {12, 14, 16, 20, 24} were {144, 196, 256, 400, 576} and {7.13×10^5, 9.73×10^5, 1.28×10^6, 1.98×10^6, 2.84×10^6}, respectively. Parts (a) and (b) show the results for the B21-based models of the Y- and Δ-model structures respectively, while parts (c) and (d) show the corresponding relations for the CPS3-based models.

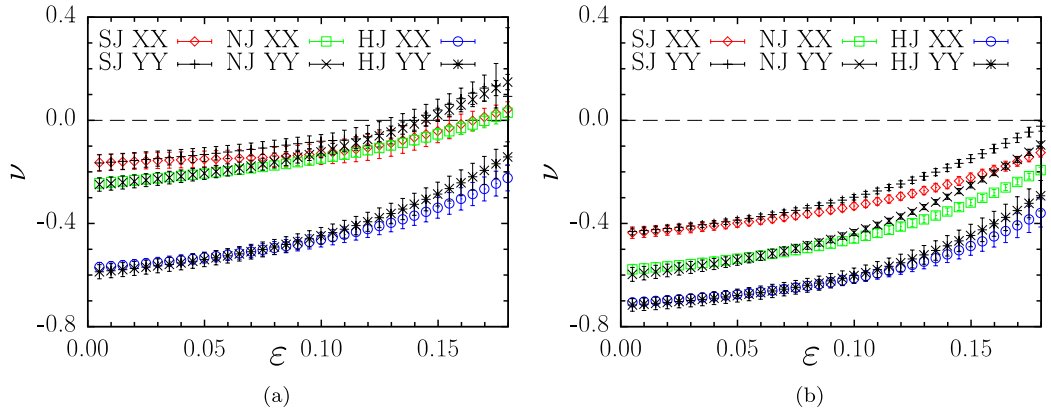

Figure 10. The Poisson's ratios of the Y-model structures (a) and the Δ-model structures (b). Disordered honeycombs and kagomé-like structures of size 16 × 16 were first compressed biaxially by 15%. The number of structures used to calculate averages and errors was varied between 8 and 12. Stretching in the x direction is represented by open symbols (diamonds for soft, squares for normal, and circles for hard joints) and in the y direction by various crosses (pluses for soft, × for normal, and stars for hard joints). The errors, marked by vertical bars, are not very different from the symbol sizes.

was expected based on theoretical considerations of angle preserving models [32, 54]. Secondly, models with Δ-joints give lower effective Poisson's ratios than those with Y-joints. In consequence, Δ-joints made of harder material give the lowest effective Poisson's ratios. These two observations can be helpful in designing foams of required properties.

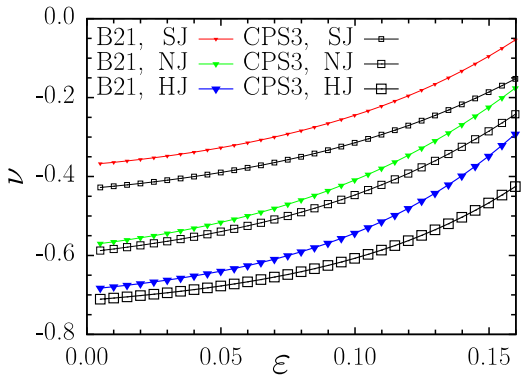

Figure 11. Comparison of the B21-based model (i.e. the one-dimensional Timoshenko beam model, represented by filled triangles) with the CPS3-based plane stress element model (represented by open squares). The sizes of the symbols grow with increasing hardness of the joints. The studied structures were of the Δ-model. It should be recalled that the beam-based model suffers from the lack of a contact treatment.

The averages and standard deviations presented in figure 10 were calculated for the various sets of samples studied, containing between 8 and 12 structures in each. It can be seen that uniaxial stretching is accompanied by increase of the Poisson's ratio. It is interesting that for Y-joints (figure 10) one observes rather small differences between the Poisson's ratios of soft and normal joints. This difference is a few times smaller than the analogous difference between normal and hard joints. This is in contrast to the Δ-joints for which the analogous differences are close to each other and not small.

In figure 11 the values of the Poisson's ratio obtained using models based on the Timoshenko beam formalism (triangles) and plane stress-based models (squares) are compared. The model utilizing beam elements was not able to handle the contact of certain elements getting close to each other when the specimen was compressed. The analysis was performed for structures of size 16×16 with high disorder introduced ($f = 0.45$). The size of the mesh was chosen in such a way that the maximum distance between neighboring m-nodes was less than or equal to $0.01D$. The plots indicate that the beam-based model describes the changes of Poisson's ratio qualitatively, being quantitatively within about 10–30% accuracy. The accuracy is best for normal joints and worst for soft ones.

Thus, the beam models are promising candidates for preliminary, qualitative analysis of the mechanical properties of cellular structures. Additionally, taking into account the relatively (compared to the plane-stress model) lower number of degrees of freedom, it is clear that the analysis utilizing beams requires much less computational effort in terms of CPU time (about two orders of magnitude for the typical structures studied in this work) and memory (about an order of magnitude for typical structures). Nevertheless, it is crucial to remember that the quantitative analysis should be based on the non-simplified continual model.

5. Conclusions

Two 2D models of disordered foam structures, the so called Y-model and Δ-model, were investigated by computer simulations using the finite element method. It has been shown that both the models reveal the effect of *compression-induced auxeticity*. The simulations performed for an initial compression of up to 20% prove that the stronger the initial compression is, the larger the auxetic effect is. The simulation results indicate that the Δ-model, for which Poisson's ratios as low as $\nu \approx -0.75$ have been reached for joints ten times harder than the ribs, shows lower values of the Poisson's ratio than the Y-model, for which the lowest values of ν were close to -0.6 for the hardest joints studied. However, it is worth stressing that for joints of the same hardness as the ribs or softer, the Poisson's ratio of the Δ-model is *two* times more negative than its value for the Y-model. These results show that large compression of initial foam structures and extensive and rigid joints are favorable for strongly auxetic behavior.

The results of FEM simulations performed with fine meshes (CPS3) have been compared with the corresponding results of simulations using one-dimensional (1D) Timoshenko beams (B21). The latter computations were performed without proper treatment of new contacts appearing at buckling, i.e. different ribs did not know if/when they touched each other. The B21 simulations were faster by about two orders of magnitude than the CPS3 ones and used less memory by about one order of magnitude than the latter ones. Figure 11 convinces one that the approach utilizing purely 1D elements (beams) is capable of handling qualitatively both of the studied models in the preliminary stage analysis; the errors are of the order of 10–30%.

It is worth adding that the models studied allow not only for very easy introduction of modifications, which can be of structural, topological and material type, but also for generalization to 3D. The introduction of modifications is crucial when investigating the mechanisms ruling the discussed effect. The present study, restricted to 2D systems with structural and material changes only, clearly indicates the importance of the joint-to-rib stiffness ratio. The harder the joints are, the lower the Poisson's ratio of auxetic structures *spontaneously formed* by compression of common ones is.

Acknowledgments

This work was supported by the (Polish) National Centre for Science under the grant NCN 2012/05/N/ST5/01476. Some of the simulations were performed at the Poznań Supercomputing and Networking Center (PCSS). This research was also supported by the PL-Grid Infrastructure. Two of the authors (AAP and KWW) are grateful to Professor Ryszard Czajka for creating excellent conditions for this work at the Department of Technical Physics of the Poznań University of Technology. One of the authors (AAP) thanks M.Sc. Eng. Michał Hermanowicz for making his computational resources available for processing and storage of some data files.

References

[1] Gibson L J and Ashby M F 1999 *Cellular Solids: Structure and Properties* (*Cambridge Solid State Science Series*) 2nd edn (Cambridge: Cambridge University Press)
[2] Bardenhagen S G, Brydon A D and Guilkey J E 2005 *J. Mech. Phys. Solids* **53** 597–617
[3] Gdoutos E E, Daniel I M and Wang K A 2002 *Composites* A **33** 163–76
[4] Viot P 2009 *Int. J. Impact Eng.* **36** 975–89
[5] McDonald S A, Ravirala N, Withers P J and Alderson A 2009 *Scr. Mater.* **60** 232–5
[6] Bouix R, Viot P and Lataillade J 2009 *Int. J. Impact Eng.* **36** 329–42
[7] Laroussi M, Sab K and Amina A 2002 *Int. J. Solids Struct.* **39** 3599–623
[8] Okumura D, Okada A and Ohno N 2008 *Int. J. Solids Struct.* **45** 3807–20
[9] McDonald S A, Dedreuil-Monet G, Yao Y T, Alderson A and Withers P J 2011 *Phys. Status Solidi* b **248** 45–51
[10] Schwerdtfeger J, Wein F, Leugering G, Singer R F, Körner C, Stingl M and Schury F 2011 *Adv. Mater.* **23** 2650–4
[11] Zhu H X, Knott J F and Mills N J 1997 *J. Mech. Phys. Solids* **45** 319–25
[12] Zhu H X, Mills N J and Knott J F 1997 *J. Mech. Phys. Solids* **45** 1875–99
[13] Zhu H, Hobdell J R and Windle A H 2000 *Acta Mater.* **48** 4893–900
[14] Zhu H, Thorpe S and Windle A 2006 *Int. J. Solids Struct.* **43** 1061–78
[15] Gong L, Kyriakides S and Jang W 2005 *Int. J. Solids Struct.* **42** 1355–79
[16] Gong L, Kyriakides S and Jang W 2005 *Int. J. Solids Struct.* **42** 1381–99
[17] Roberts A P and Garboczi E J 2001 *Acta Mater.* **49** 189–97
[18] Roberts A P and Garboczi E J 2002 *J. Mech. Phys. Solids* **50** 33–55
[19] Brydon A, Bardenhagen S, Miller E and Seidler G 2005 *J. Mech. Phys. Solids* **53** 2638–60
[20] Elliott J A, Windle A H, Hobdell J R, Eeckhaut G, Oldman R J, Ludwig W, Boller E, Cloetens P and Baruchel J 2002 *J. Mater. Sci.* **37** 1547–55
[21] Lakes R S 1987 *Science* **235** 1038–40
[22] Grima J N, Attard D, Gatt R and Cassar R N 2009 *Adv. Eng. Mater.* **11** 533–5
[23] Landau L D and Lifshitz E M 1986 *Theory of Elasticity* (*Teoretičeskaja fizika*) (Oxford: Pergamon)
[24] Evans K E 1991 *Endeavour* **15** 170–4
[25] Almgren R 1985 *J. Elasticity* **15** 427–30
[26] Wojciechowski K W 1987 *Mol. Phys.* **61** 1247–58
[27] Bathurst R J and Rothenburg L 1988 *Int. J. Eng. Sci.* **26** 373–83
[28] Wojciechowski K W 1989 *Phys. Lett.* A **137** 60–4
[29] Caddock B D and Evans K E 1989 *J. Phys. D: Appl. Phys* **22** 1877–82
[30] Evans K E, Nkansah M A, Hutchinson I J and Rogers S C 1991 *Nature* **353** 124
[31] Lakes R S 1991 *J. Mater. Sci.* **26** 2287–92
[32] Rothenburg L, Berlin A I and Bathurst R J 1991 *Nature* **354** 470–2
[33] Milton G W 1992 *J. Mech. Phys. Solids* **40** 1105–37
[34] Wei G 1992 *J. Chem. Phys.* **96** 3226–33
[35] Keskar N R and Chelikowsky J R 1993 *Phys. Rev.* B **48** 16227–33
[36] Boal D H, Seifert U and Shillcock J C 1993 *Phys. Rev.* E **48** 4274–83
[37] Wojciechowski K W 1995 *Mol. Phys. Rep.* **10** 129–36
[38] Prall D and Lakes R S 1996 *Int. J. Mech. Sci.* **39** 305–14
[39] Larsen U D, Sigmund O and Bouwstra S 1997 *J. Microelectromech. Syst.* **6** 99–106
[40] Schärer U and Wachter P 1997 *Physica* B **230** 721–4
[41] Baughman R H, Shacklette J M, Zakhidov A A and Stafstrom S 1998 *Nature* **392** 362–5
[42] Novikov V V and Wojciechowski K W 1999 *Phys. Solid State* **41** 1970–5
[43] Ishibashi Y and Iwata M 2000 *J. Phys. Soc. Japan* **69** 2702–3
[44] Grima J N and Evans K E 2000 *J. Mater. Sci. Lett.* **19** 1563–5
[45] Kimizuka H, Kaburaki H and Kogure Y 2000 *Phys. Rev. Lett.* **84** 5548–51
[46] Bowick M, Cacciuto A, Thorleifsson G and Travesset A 2001 *Phys. Rev. Lett.* **87** 148103
[47] Alderson A and Evans K E 2002 *Phys. Rev. Lett.* **89** 225503
[48] Vasiliev A A, Dmitriev S V, Ishibashi Y and Shigenari T 2002 *Phys. Rev.* B **65** 094101
[49] Pikhitsa P V 2004 *Phys. Rev. Lett.* **93** 015505
[50] Ruzzene M and Scarpa F 2005 *Phys. Status Solidi* b **242** 665–80
[51] Ting T C T and Barnett D M 2005 *J. Appl. Mech.* **72** 929–31
[52] He C, Liu P, McMullan P J and Griffin A C 2005 *Phys. Status Solidi* b **242** 576–84
[53] Norris A N 2006 *Proc. R. Soc.* A **462** 3385–405
[54] Lakes R S and Wojciechowski K W 2008 *Phys. Status Solidi* b **245** 545–51
[55] Spadoni A, Ruzzene M, Gonella S and Scarpa F 2009 *Wave Motion* **46** 435–50
[56] Schwerdtfeger J, Heinl P, Singer R F and Körner C 2010 *Phys. Status Solidi* b **247** 269–72
[57] Chrzanowska A 2010 *Acta Phys. Pol.* B **41** 1977–89
[58] Valant M, Axelsson A K, Aguesse F and Alford N M 2010 *Adv. Funct. Mater.* **20** 644–7
[59] Pasternak E and Dyskin A V 2012 *Int. J. Eng. Sci.* **52** 103–14
[60] Prawoto Y 2012 *Comput. Mater. Sci.* **58** 140–53
[61] Lakes R S 1993 *Adv. Mater.* **5** 293–6
[62] Evans K E and Alderson A 2000 *Adv. Mater.* **12** 617–28
[63] Evans K E and Alderson K L 2000 *Eng. Sci. Educ. J.* **9** 148–54
[64] Hadjigeorgiou E P and Stavroulakis G E 2004 *CMST* **10** 147–60
[65] Ravirala N, Alderson A, Alderson K L and Davies P J 2005 *Phys. Status Solidi* b **242** 653–64
[66] Alderson A and Alderson K L 2007 *Proc. Inst. Mech. Eng.* G **221** 565–75
[67] Hassan M R, Scarpa F, Ruzzene M and Mohammed N 2008 *Mater. Sci. Eng.* A **481/482** 654–7
[68] Alderson A, Rasburn J, Evans K E and Grima J N 2001 *Membr. Technol.* **2001** 6–8
[69] Choi J B and Lakes R S 1995 *Int. J. Mech. Sci.* **37** 51–9
[70] Smith C W and Grima J N 2000 *Acta Mater.* **48** 4349–56
[71] Brandel B and Lakes R S 2001 *J. Mater. Sci.* **36** 5885–93
[72] Pastorino P, Scarpa F, Patsias S, Yates J R, Haake S J and Ruzzene M 2007 *Phys. Status Solidi* b **244** 955–65
[73] Cadamagnani F, Frontoni S, Bianchi M and Scarpa F 2009 *Phys. Status Solidi* b **246** 2118–23
[74] Horrigan E J, Smith C W, Scarpa F L, Gaspar N, Javadi AA, Berger M and Evans K E 2009 *Mech. Mater.* **41** 919–27
[75] Bianchi M, Scarpa F, Banse M and Smith C W 2011 *Acta Mater.* **59** 686–91
[76] Gatt R, Attard D, Manicaro E, Chetcuti E and Grima J N 2011 *Phys. Status Solidi* b **248** 39–44
[77] Bouakba M, Bezazi A and Scarpa F 2012 *Int. J. Solids Struct.* **49** 2450–9
[78] Scarpa F, Panayiotou P and Tomlinson G 2000 *J. Strain Anal. Eng. Des.* **35** 383–8

[79] Gaspar N, Ren X, Smith C, Grima J and Evans K 2005 *Acta Mater.* **53** 2439–45
[80] Álvarez Elipe J C and Díaz Lantada A 2012 *Smart Mater. Struct.* **21** 105004
[81] Alderson A, Alderson K L, Attard D, Evans K E, Gatt R, Grima J N, Miller W, Ravirala N, Smith C W and Zied K 2010 *Compos. Sci. Technol.* **70** 1042–8
[82] Lorato A, Innocenti P, Scarpa F, Alderson A, Alderson K L, Zied K M, Ravirala N, Miller W, Smith C W and Evans K E 2010 *Compos. Sci. Technol.* **70** 1057–63
[83] Cicala G, Recca G, Oliveri L, Perikleous Y, Scarpa F, Lira C, Lorato A, Grube D J and Ziegmann G 2012 *Compos. Struct.* **94** 3556–62
[84] Ohno N, Okumura D and Noguchi H 2002 *J. Mech. Phys. Solids* **50** 1125–53
[85] Hibbit D, Karlsson B and Sorensen P 2010 *ABAQUS/Standard Analysis User's Manual, ver. 6.10*
[86] Saiki I, Terada K, Ikeda K and Hori M 2002 *Comput. Methods Appl. Mech. Eng.* **191** 2561–85